Permanent scatterer InSAR reveals seasonal and long-term aquifer-system response to groundwater pumping and artificial recharge

John W. Bell,[1] Falk Amelung,[2] Alessandro Ferretti,[3] Marco Bianchi,[3] and Fabrizio Novali[3]

Received 4 May 2007; revised 30 July 2007; accepted 10 October 2007; published 5 February 2008.

[1] Permanent scatterer InSAR (PSInSAR™) provides a new high-resolution methodology for detecting and precisely measuring long-term and seasonal aquifer-system response to pumping and recharge. In contrast to conventional InSAR, the permanent scatterer methodology utilizes coherent radar phase data from thousands of individual radar reflectors on the ground to develop displacement time series and to produce velocity field maps that depict aquifer-system response with a high degree of spatial detail. In this study, we present the first results of a prototype study in Las Vegas Valley, Nevada, that demonstrate how this methodology can be utilized in heavily pumped groundwater basins to analyze aquifer-system response to long-term and seasonal pumping. We have developed a series of velocity field maps of the valley for the 1992–1996, 1996–2000, and 2003–2005 time periods that show that despite rising water levels associated with an artificial recharge program, long-term, residual, inelastic aquifer-system compaction (subsidence) is continuing in several parts of the valley. In other areas, however, long-term subsidence has been arrested and locally reversed. The seasonal, elastic responses to alternating pumping and recharge cycles were segregated from the long-term trends and analyzed for spatial and temporal patterns. The results show oscillations in which the maximum seasonal responses are associated with the late stages of the annual artificial recharge cycles, and that similar seasonal subsidence signals are related to summer pumping cycles. The differentiation of the seasonal response through the use of time series data further allows the estimation of elastic and inelastic skeletal storage coefficients, providing a basis for future work that could characterize the storage properties of an aquifer system with a high degree of spatial resolution.

Citation: Bell, J. W., F. Amelung, A. Ferretti, M. Bianchi, and F. Novali (2008), Permanent scatterer InSAR reveals seasonal and long-term aquifer-system response to groundwater pumping and artificial recharge, *Water Resour. Res.*, *44*, W02407, doi:10.1029/2007WR006152.

1. Purpose and Scope

[2] Many groundwater basins in the arid and semi-arid western US have experienced aquifer-system compaction, or subsidence, in response to heavy pumping. Numerous examples are found in the valleys of California, Arizona, New Mexico, and Nevada, with some of the more important case histories documented in the Santa Clara and San Joaquin Valleys of California, the basins of south-central Arizona, and in Las Vegas Valley [*Galloway et al.*, 1999]. Because much of the subsidence occurring in these heavily pumped aquifer systems is irrecoverable, resulting in a loss of aquifer storage, and because damage to engineered structures may be associated with the subsidence, it is important to groundwater managers and groundwater purveyors to understand the spatial and temporal patterns of the aquifer-system response in order to more effectively manage water resources. In this paper, we investigate aquifer-system processes using a new radar methodology and show that this is a methodology that could be widely applied to other similar groundwater basins in the western US.

[3] The application of interferometric synthetic aperture radar (InSAR) studies to hydrogeological problems has advanced rapidly during the last decade, and it is now routinely applied to a wide range of groundwater resource issues, including groundwater flow modeling, estimation of aquifer-system hydraulic properties, and facilitating improved management of groundwater resources [*Galloway and Hoffmann*, 2006]. The application of permanent scatterer InSAR (PSInSAR™) now provides an additional methodology that allows for greater resolution and accuracy in the detection of ground movement produced by aquifer-system withdrawals and recharge.

[4] In this paper, we present the first results of a PSInSAR™ prototype study in Las Vegas Valley that focuses on the pattern and timing of aquifer-system response to pumping and artificial recharge. First, we present a set of PSInSAR™-derived ground deformation maps that

[1] Nevada Bureau of Mines and Geology, University of Nevada, Reno, Nevada, USA.
[2] Rosenstiel School of Marine and Atmospheric Science, University of Miami, Miami, Florida, USA.
[3] Tele-Rilevamento Europa, Via Vittoria Colonna, Milan, Italy.

0043-1397/08/2007WR006152$09.00

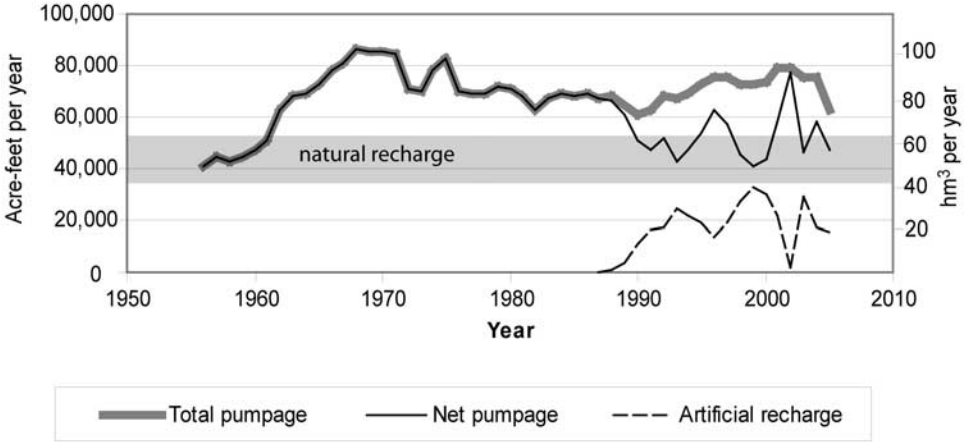

Figure 1. Volume of total pumpage, artificial recharge, and net groundwater pumpage in Las Vegas Valley, 1950–2005. Artificial recharge program begun by Las Vegas Valley Water District in the late 1980s has resulted in reduced net pumpage each year, except for 2002. (Robert Coache, Nevada State Engineer's Office, unpub. data).

allow for a greater resolution in displacement time series than previously available through the use of conventional InSAR. Velocity and acceleration/deceleration analyses permit a close examination of patterns of subsidence and uplift responding to rising water levels during the study period. We evaluate the residual compaction that is occurring despite rising water levels, then examine the nature of the seasonal subsidence and uplift signals that are superimposed on the long-term subsidence trends. The magnitude and timing of the seasonal signal is segregated and correlated to water-level fluctuations to characterize aquifer-system response patterns and to further refine measurements of aquifer storage properties. Finally, we use the PSInSAR™ results to better resolve aquifer-system complexities and to explain the observed lack of correlation between pumping/recharge centers and the principal zones of aquifer-system response.

2. Background

[5] The Las Vegas metropolitan area led the US in population growth during the 1990s, increasing from 852,000 in 1990 to more than 1.5 million in 2000, and it has continued to grow at a rate of about 6000 people per month. Although natural springs historically provided water to this arid valley (12–20 cm/a average annual precipitation), groundwater pumping was initiated in 1905 to support early development in the valley, and by 1960 groundwater withdrawals had reached about 49 hm^3 (40,000 acre-ft) per year (Figure 1). Total pumpage increased through 1970 reaching a peak of 106 hm^3 (86,000 acre-ft) per year; in 1972 groundwater resources began to be supplemented by importation of Colorado River water and a stabilization of pumping rates was reached at about 92 hm^3 (75,000 acre-ft) per year. However, since the 1960s, the annual groundwater withdrawals have consistently exceeded the estimated natural recharge rates of 43–68 hm^3 (35,000–55,000 acre-ft) per year [*Maxey and Jameson*, 1948; *Donovan and Katzer*, 2000]. Beginning in the late 1980s the Las Vegas Valley Water District initiated an artificial recharge program that injected imported Colorado River water into the principal aquifers during the winter season, with the annual recharge rate reaching a peak of 39 hm^3 (32,000 acre-ft) per year by 1999 (Figure 1). The effect of the artificial recharge has been to reduce the net annual pumpage to about 55 hm^3 (45,000 acre-ft) per year.

[6] The long-term effects of continued overdrafting of the groundwater system through the early 1990s included the depressurization of the aquifer system and the regional decline of water levels as much as 90 m by 1990 (Figure 2a). Since initiation of the artificial recharge program, water levels have stabilized and recovered by as much 30 m (Figure 2b), but owing to the effects of the long-term depressurization of the fine-grained deposits, compaction of the aquifer system has continued and land subsidence of more than 1.7 m has been measured through 2000 [Figure 2c; *Bell et al.*, 2002].

[7] Although subsidence had been monitored throughout the valley by conventional methodologies since 1935, the use of InSAR first revealed the spatial and temporal details of the regional aquifer-system response to pumping, including the influence of structural (fault) controls on aquifer response, and the reduction in subsidence rates during the late 1990s [*Amelung et al.*, 1999]. Subsequent InSAR studies showed that seasonal response to pumping and recharge could be segregated and utilized to gain further insights into aquifer-system response, including characterization of elastic storage properties [*Hoffmann et al.*, 2001].

3. The PSInSAR™ Methodology

[8] Conventional, differential, satellite repeat-pass InSAR is a methodology in which two radar scenes acquired over the same area at different times provide radar phase information that allows detection and measurement of sub-centimeter-scale ground movement in the form of a phase-change interferogram. The successful application of conventional InSAR to ground deformation studies is typically dependent upon a number of variables: availability of archival radar data to bracket the timing of the deformation event; suitable satellite baseline geometry; retrieval of

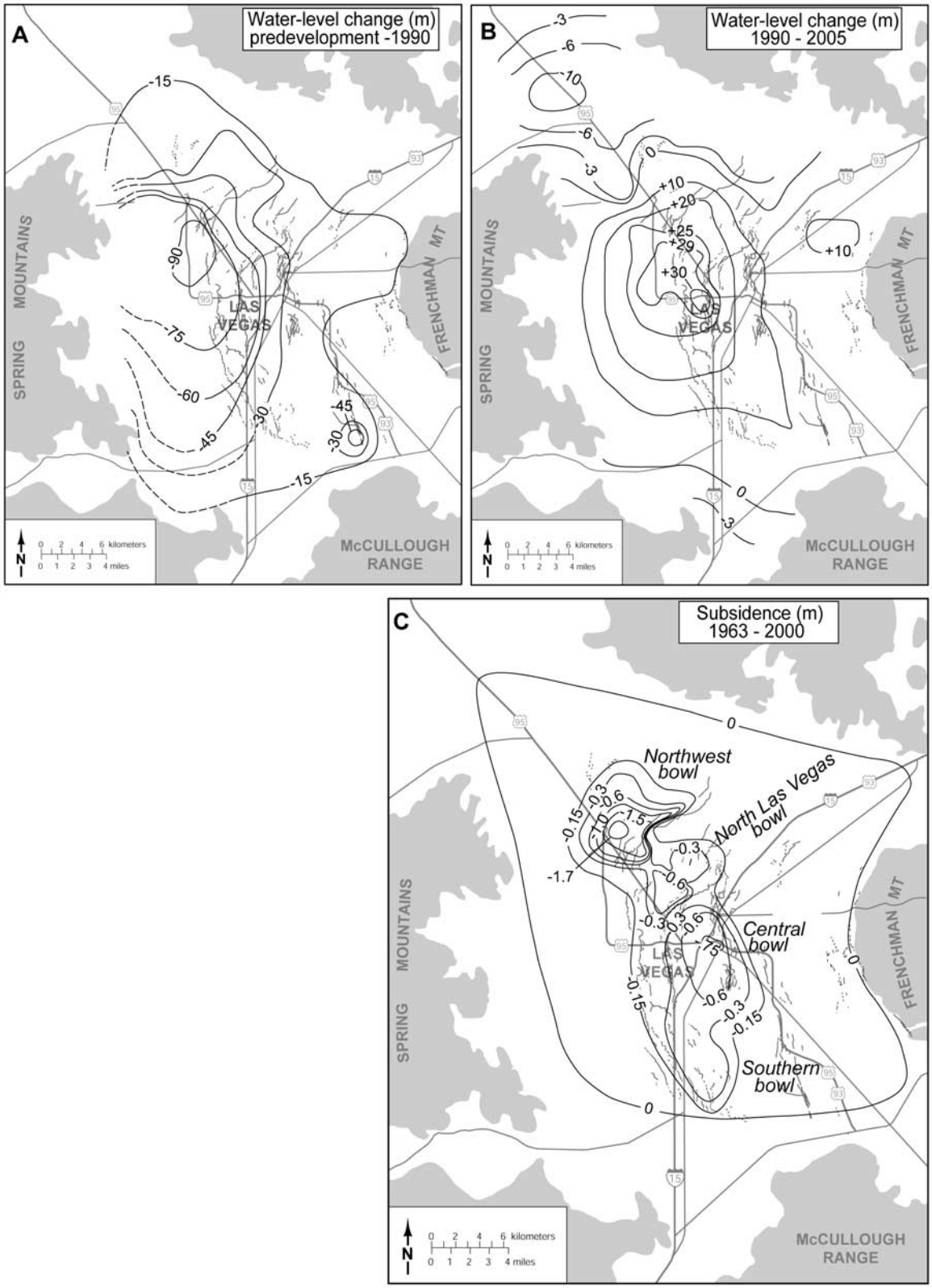

Figure 2. Water-level change and land subsidence in Las Vegas Valley. All contours in meters. (a) Water-level change in Las Vegas Valley due to groundwater pumping, pre-development to 1990 [*Burbey*, 1995]. (b) Water-level change, 1990–2005 [*Las Vegas Valley Water District*, 2005]. (c) Land subsidence in Las Vegas Valley, 1963–2000 [*Bell et al.*, 2002].

coherent phase data, and identification and removal of phase changes unrelated to ground deformation, such as topography, residual satellite orbital errors, and atmospheric artifacts [cf., *Hanssen*, 2001]. Measurement of the radar phase change is made on a pixel-resolution ($\sim$80 m^2) basis with a full-cycle of phase change equivalent to one-half of the radar wavelength (5.6 cm for C-band radar), or 2.8 cm of radar line-of-sight (LOS) displacement.

[9] In contrast, the permanent scatterer (PS) methodology utilizes the identification and exploitation of individual radar reflectors, or permanent scatterers, that are smaller than the resolution pixel cell and that remain coherent over long time intervals in order to develop displacement time series [*Ferretti et al.*, 2001]. The resolution that is achieved by the identification of these PS targets effectively results in the creation of a data set consisting of many tiny "benchmarks". The advantages of the PS methodology are several: 1) good phase coherence is obtained from nearly all radar scenes regardless of geometrical baseline (perpendicular separation of the satellite positions), and long baseline interferometry with up to 1.6 km separation can be carried out; 2) all available radar scenes in the archive can be exploited; and 3) atmospheric phase contributions can be estimated and removed from the deformation phase signal.

[10] A multiinterferogram approach, optimally incorporating more than 30 radar scenes, is used to identify consistently coherent targets throughout the entire time series, and to derive accurate phase-change data for each target. This is facilitated through the use of "zero-baseline steering" which estimates the geometric phase contribution of different-baseline radar scenes and corrects this phase component relative to a reference or "master" scene. The identification of stable scatterers is carried out by analyzing the time series of the radar amplitude values, and by looking for persistent, bright radar reflectors, most commonly fixed dihedral structures, such as buildings or other similar objects. False phase-change signals (artifacts) due to atmospheric contributions are estimated through the use of an atmospheric phase screen (APS) analysis. Atmospheric phase contributions are determined for each radar acquisition and subtracted from the total phase residuals derived from the interferometry process.

4. Approach

[11] Two independent satellite data sets obtained from the European Space Agency were available for the study. We used 50 ERS-satellite acquisitions in a descending track mode taken over Las Vegas Valley between April 1992 and August 2000, and 19 ENVISAT-satellite acquisitions (all available ENVISAT acquisitions at the time of the study) in a descending track mode taken between October 2002 and May 2005 for the PS time series analyses. After APS estimation and correction to each acquisition, the two data sets were processed with the PSInSAR™ algorithm [*Ferretti et al.*, 2001] to derive deformation phase data for each PS, to calculate the radar line-of-sight (LOS) displacement of each PS relative to the "master" acquisitions (28 February 1997 for the ERS data and 27 February 2004 for the ENVISAT data), and to develop the average velocity fields from the two independent data sets. Because of the steep ($\sim$23°) look-angle for ERS and ENVISAT radar data, we assume that measured LOS displacements are vertical [cf., *Hoffmann et al.*, 2001].

[12] A 40 km $\times$ 40 km framework area containing 500,000 PS targets was initially analyzed (Figure 3). The areas exhibiting subsidence are visible in the Northwest subsidence bowl and along the north-south axis of the valley. The strong structural influence is very evident in this framework velocity field map, with the subsiding areas sharply bounded by faults, in good agreement with the earlier conventional InSAR results [*Amelung et al.*, 1999; *Hoffmann et al.*, 2001; *Bell et al.*, 2002].

[13] A 20 km $\times$ 20 km subset area containing 90,000 PS data points and centered over the Northwest subsidence bowl-Eglington fault area was selected from the framework area to study in greater detail the aquifer-system response to temporal variations in groundwater pumping and artificial recharge. This area has exhibited the greatest subsidence since the 1960s (Figure 2c), although the principal areas of groundwater pumping and recharge are located in the adjoining area to the south. Displacements for PS points in the Eglington fault area were determined, independent time series for the ERS and ENVISAT data sets were developed, non-linear motion of each time series (seasonal variation) was evaluated, and average displacement velocity maps were produced. Temporal windows were selected in order to examine subsidence trends occurring during the periods 1992–1996 (greatest subsidence rates), 1996–2000 (reduced subsidence rates), and 2003–2005 (reduced subsidence rates with largest water-level recoveries). The temporal comparison further allowed the estimation of an acceleration field for the time period covered by the ERS data set. Because water levels in Las Vegas Valley exhibit large seasonal fluctuations, the time periods were selected to be consistent with seasonality.

[14] Individual PS time series were analyzed for seasonal and long-term trends to identify spatial patterns, to compare with water-level fluctuations, and to characterize the elastic and inelastic storage properties of the aquifer system.

5. Accuracy of the PSInSAR™ Methodology

[15] The accuracy of the PSInSAR™ methodology can be sub-centimeter-scale if a sufficient number of acquisitions are utilized in the PS analysis [*Ferretti et al.*, 2001]. In a controlled experiment, *Ferretti et al.* [2007] found a maximum difference of 3 mm between the PS displacement results and the actual movement of the ground reflector. Owing to the large time gap between the two data sets in our study, ERS and ENVISAT acquisitions could not be efficiently co-processed, so separate time series were developed.

[16] To test the accuracy of the PS results from Las Vegas Valley, we compared the results with independent vertical displacement data from a borehole extensometer operated by the US Geological Survey in the Northwest subsidence bowl [*Pavelko*, 2000]. Figure 4 shows a comparison between the 1995–2005 displacements recorded by the extensometer in the depth range of 4–244 m (total displacement 45 mm) and the PS time series data for an ERS target (DW197) and an ENVISAT target (BU292) adjacent to the extensometer (Figure 5a). Between 1995 and 2000, PS displacements replicate both the seasonal and

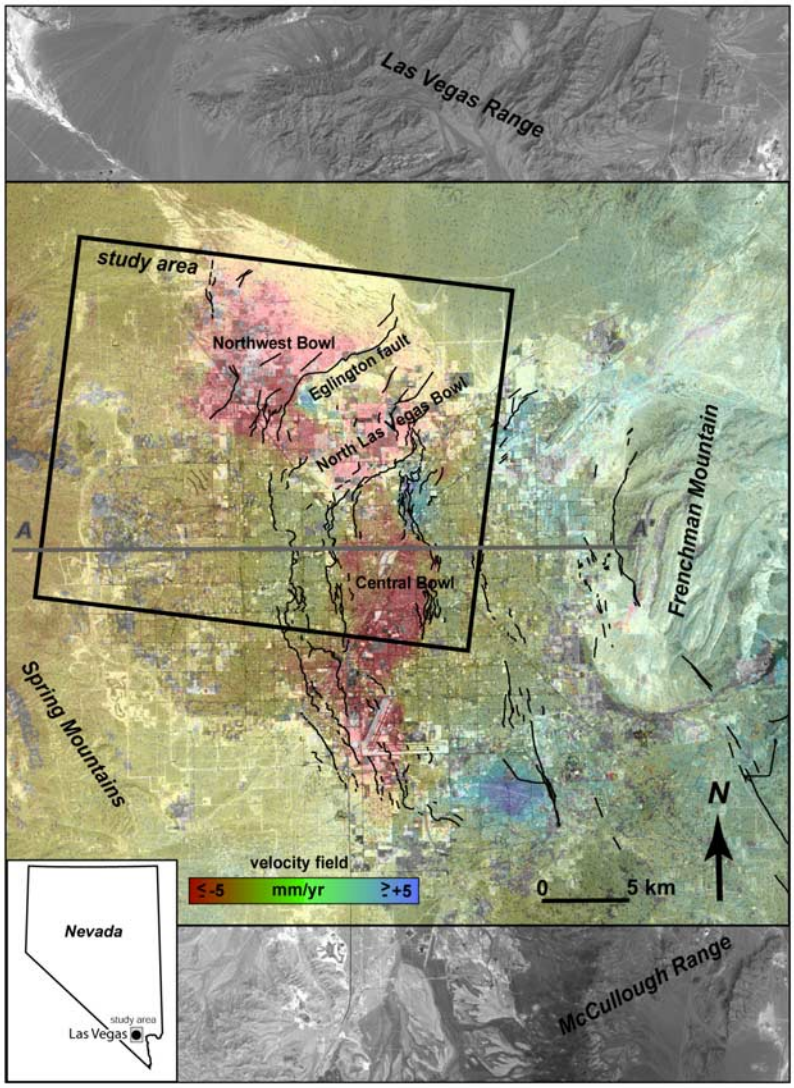

Figure 3. Permanent scatterer velocity map of a 40 × 40 km framework area in Las Vegas Valley for the period 1996–2000 showing generalized PS rates; red areas denote subsidence and blue areas, uplift. Total number of PS targets in the framework area is more than 500,000. Study area (inset box) is a smaller subset (90,000 targets) of the PS data covering the Northwest part of the valley. Cross section A-A′ shown in Figure 6.

long-term trends of the extensometer with an accuracy of about 3–5 mm, and the long-term average PS velocity and the compaction rates are very close: 4.6 mm/a and 5.0 mm/a, respectively. In a similar conventional InSAR test by *Hoffmann et al.* [2001], the seasonal displacements were found to be larger than the extensometer results, although the long-term InSAR trend was comparable to the extensometer record. They attributed the seasonal differences to compaction occurring below the 244-m depth of the extensometer. Our comparison of the PS results and the extensometer record shows that while the long-term trends are also similar, we found less variation in the seasonal change than described by *Hoffmann et al.* [2001].

[17] The smaller ENVISAT data set shows more scatter than the larger ERS data set, and the average 2002–2005 subsidence rate is lower than the extensometer compaction rate: 1.9 mm/a versus 4.0 mm/a, respectively. We regard the ENVISAT results as preliminary, containing greater uncertainties than the ERS results; the uncertainties of the ENVISAT data will improve as more acquisitions become available.

6. Results and Discussion

6.1. Time Series Velocities and Water-Level Change

[18] The time series results were separated into three temporal windows in order to compare early ERS (1992–1996), late ERS (1996–2000), and recent ENVISAT (2003–2005) results with well-constrained water-level data for the same time periods (Figure 5). Quarterly water-level data provided by the Las Vegas Valley Water District for 1992–1996 (50 wells) and 1996–2000, 2003–2005 (100 wells) were used to produce water-level change maps for the study area. Diagrammatic hydrostratigraphic relations for the study area are shown in Figure 6.

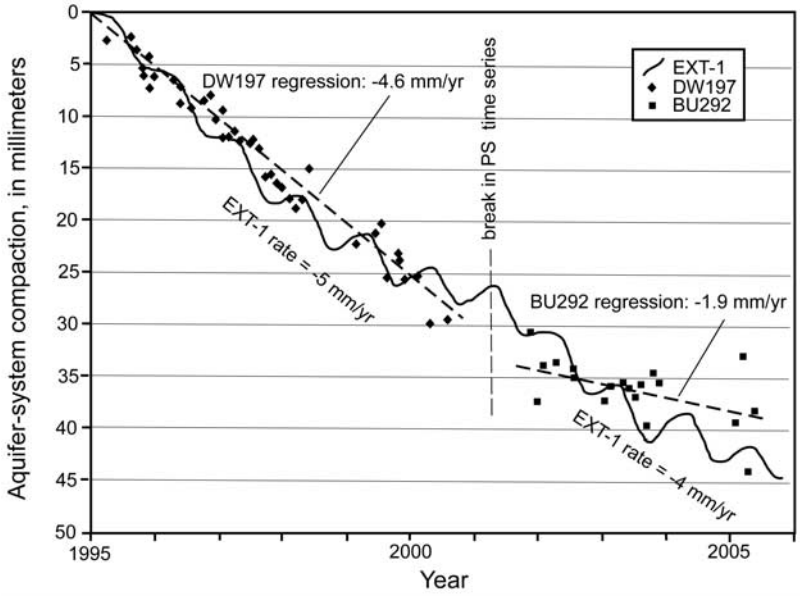

Figure 4. Comparison of compaction recorded at US Geological Survey borehole extensometer EXT-1 (see Figure 5 for location) with permanent scatterer ERS results for 1995–2000 (PS target DW 197) and ENVISAT 2002–2005 (PS target BU 292). Because the two time series are processed separately, a break occurs between the ERS and ENVISAT data. Subsidence rates were calculated from average long-term trends of the extensometer records, and from linear regressions calculated for the PS data. (Extensometer data provided by M. Pavelko, US Geological Survey).

[19] A comparison of the three temporal windows shows progressively reduced time series velocities (reduced subsidence rates) related to consistently rising water levels. Between spring 1992 and spring 1996 (Figure 5a), subsidence in the Northwest bowl occurred at a maximum average rate of 2–3 cm/a, consistent with earlier conventional InSAR interpretations and conventional geodetic data [*Amelung et al.*, 1999; *Bell et al.*, 2002]. Water levels during this period rose by more than +10 m south of the subsidence bowl in the areas of artificial recharge, but continued to decline by as much as −5 m within the bowl, indicating that the Northwest bowl continued to be a zone of primary compaction. Between spring 1996 and spring 2000 (Figure 5b), average velocities in the Northwest bowl had declined to 1–2 cm/a as water levels continued to rise by as much as +10 m, including within the Northwest bowl. By the spring 2003 to spring 2005 period (Figure 5c), maximum subsidence rates in the Northwest bowl had decreased to 5–10 mm/a, and all areas exhibited water level rise except for a newly developed area in the extreme northwest portion of the study area.

[20] The PS results show that the Northwest bowl continued to be the most actively subsiding portion of the aquifer system as recently as 2005. Maximum subsidence rates in the Northwest bowl prior to 1990 were on the order of 5 cm/a [*Bell et al.*, 2002]. The PS data show that these rates had decreased to less than 3 cm/a during the 1992–1996 period, and yet lower rates in subsequent years. PS target A (Figures 5a, 7a) is located near the center of the bowl where as much as 1.7 m of compaction has been measured with a maximum pre-1990 subsidence rate of 5.5 cm/a (Figure 2b). Between 1992–1996, target A showed a subsidence rate of 2.7 cm/a, declining to 1.8 cm/a between 1996–2000 with an average 1992–2000 rate of 2.1 cm/a. The PS data for 2003–2005 (PS target B; Figure 7b) show a further rate reduction to 6 mm/a. Locally, PS data can also be compared with conventional benchmark data records. PS target C (Figure 7c) is located at the site of USGS benchmark R169 (Figure 5a) which exhibited a geodetically measured subsidence rate of 4.8 cm/a prior to 1990. Between 1992–1996, the PS target at R169 showed a subsidence rate of 2.3 cm/a, declining to 1.3 cm/a between 1996–2000, with an average 1992–2000 rate of 1.7 cm/a. The rate declined further to 0.56 cm/a between 2003–2005 (PS target D; Figure 7d).

[21] In contrast to earlier findings [*Hoffmann et al.*, 2001], we find that residual subsidence continued during all three time periods, although in progressively lesser amounts, as water levels rose. In the 1992–1996 period, subsidence of as much as 10–20 mm/a continued in a broad zone extending from the east side of the Valley View fault north to the Eglington fault, an area exhibiting water-level rise between 0–10 m. Beginning in the 1996–2000 period, water levels throughout the study area had stabilized or recovered by as much as +5–10 m with the areas of continued compaction remaining similar to the 1992–1996 period (such as PS target E in the Central subsidence bowl; Figure 7e), indicating that subsidence was residual. Water levels continued to decline only in a localized portion of the Northwest subsidence bowl. By the 2003–2005 period, water levels had risen throughout the study area and all subsidence was residual.

[22] During these same time periods, rising water levels also produced increasing aquifer-system recovery (uplift). During the spring 1992 to spring 1996 period, uplift is visible in a localized (1–2 km) zone on the southeast side of

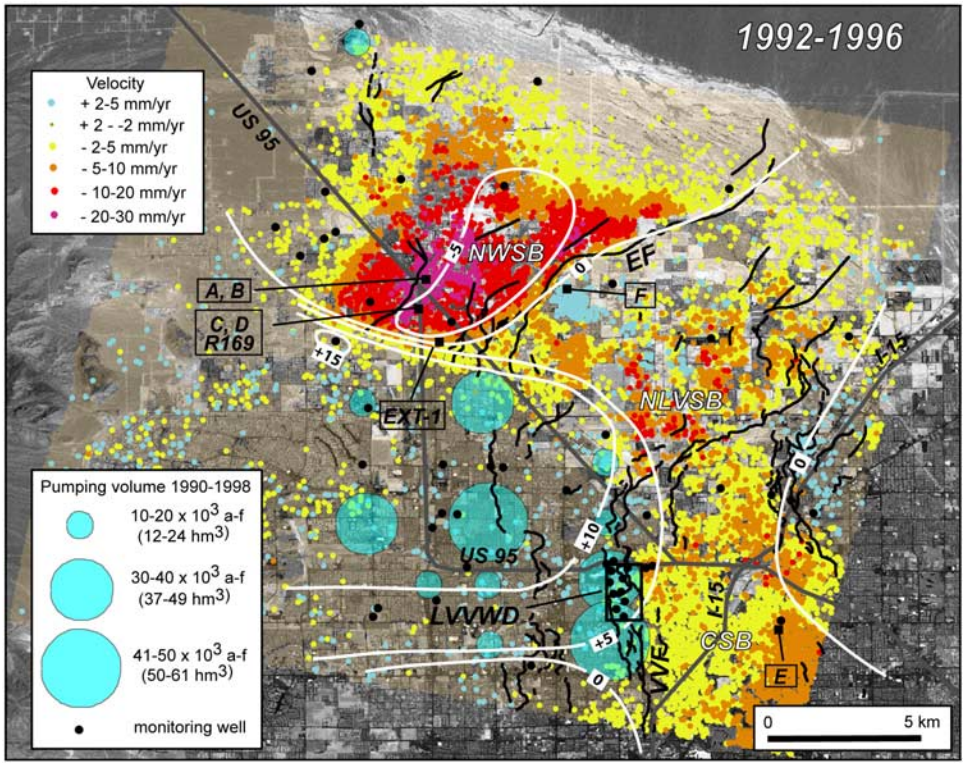

Figure 5a. Permanent scatterer velocity maps showing target velocities in mm/a for study area in northwest portion of Las Vegas Valley. On all figures: NWSB, Northwest subsidence bowl; NLVSB, North Las Vegas subsidence bowl; CSB, Central subsidence bowl; EF, Eglington fault; VVF, Valley View fault; LVVWD, Las Vegas Valley Water District; EXT-1, extensometer location. Water-level change shown as white contours in meters, derived from water-level data points (black dots). Total PS target data set shown by light brown data points with values of −2 to +2 mm/a; PS targets discussed in Figure 7 identified by letters. Faults shown as black lines. (Water level data provided by the Las Vegas Valley Water District/Southern Nevada Water Authority). (a) Permanent scatterer velocity map from ERS data for the period 21 April 1992 to 18 April 1996 and water-level change for the period March 1992 to April 1996. Total pumpage for 1990–1998 shown by light blue circles (pumping data provided by the Las Vegas Valley Water District/Southern Nevada Water Authority).

the Eglington fault, with uplift rates of as much as +5 mm/a (PS target F; Figure 7f). By spring 1996 to spring 2000, the area of uplift in this zone had expanded and the rate increased to between +5–10 mm/a (PS target G; Figure 7g). Between spring 2003 and spring 2005, the principal uplift area had shifted to the east where an 8 km long, linear zone extending south from the Eglington fault to the Las Vegas Valley Water District locally exhibited uplift velocities of more than +10 mm/a (PS target H; Figure 7h). Lesser amounts of uplift on the order of +2–5 mm/a are also broadly distributed throughout the study area (blue PS targets on Figure 5c).

[23] The PS results also show that the aquifer-system response in the North Las Vegas bowl has been reversed, the only such area we have recognized to date. This area historically exhibited as much as 60 cm of subsidence (Figure 2c). The PS data in the bowl show residual subsidence rates of more than 1 cm/a between 1996–2000 (PS target I; Figure 7i). By 2003–2005, the residual subsidence had ceased and the area was undergoing aquifer-system uplift at a rate of as much as +1 cm/a (PS target J; Figure 7j).

[24] The combined 1992–1996–2000–2005 time series reflects a gradual decline in subsidence rates, a general observation that we have also made in earlier studies [*Bell et al.*, 2002], but here clearly illustrated by diminishing velocities. On the basis of comparison of ERS velocity change between 1992–1996 and 1996–2000 for the same PS targets, an acceleration map (Figure 8) shows that aquifer-system compaction in the three principal subsidence bowls has been decelerating at an average rate of more than 1 mm/a^2. One small area in the northeast part of the study area has been accelerating.

6.2. Spatial Pattern of Aquifer-System Response

[25] As we noted in earlier studies [*Amelung et al.*, 1999; *Bell et al.*, 2002], the areas of maximum aquifer-system compaction are offset to the east from the zones of maximum pumping and maximum water-level decline occurring until 1990 (Figure 2a). Similarly, the areas of maximum aquifer-system recovery are offset to the east from the areas of maximum water-level rise occurring since 1990: the broad linear zone of uplift seen in the 2003–2005 data lies to the east of the principal area of artificial recharge where

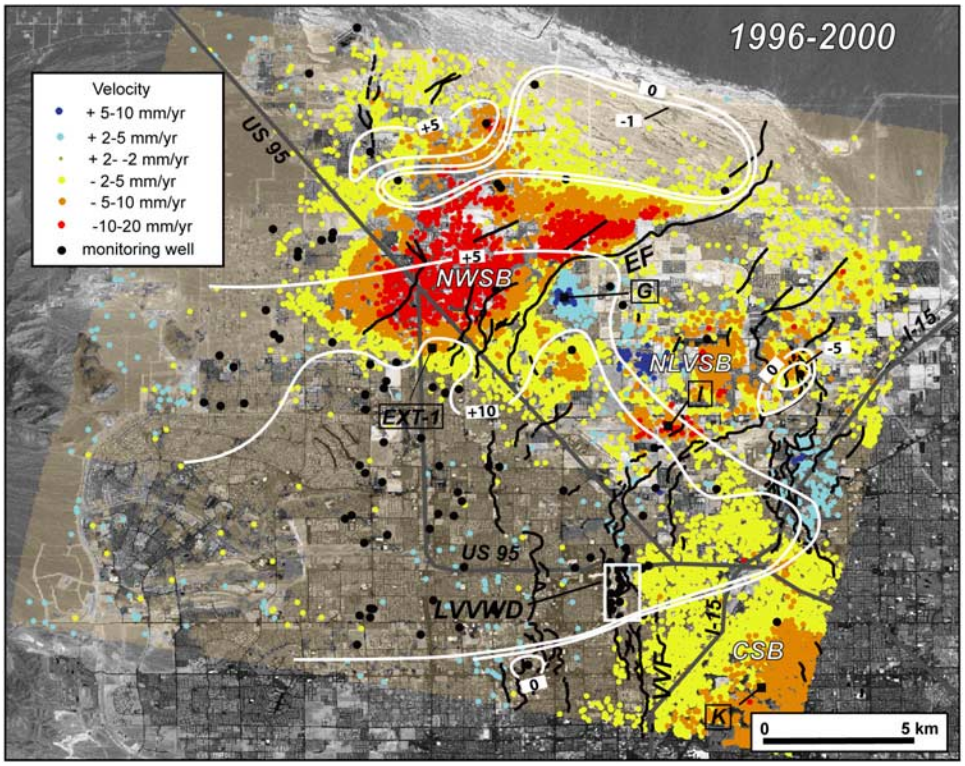

Figure 5b. Permanent scatterer velocity map from ERS data for the period 18 April 1996 to 28 April 2000 and water-level change for the period April 1996 to May 2000.

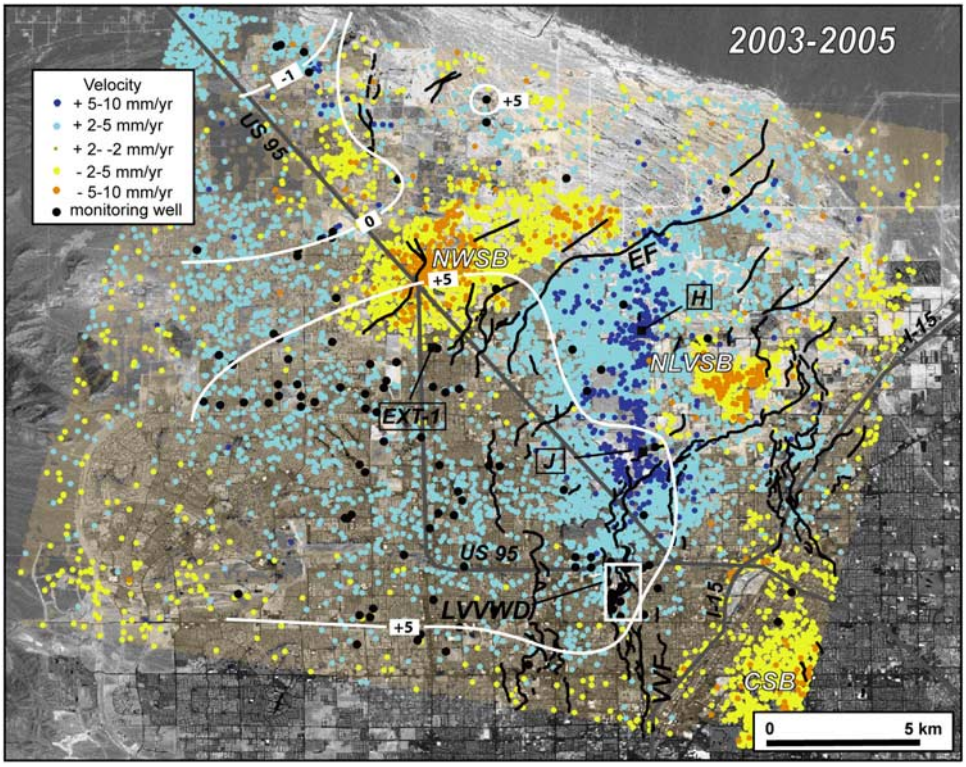

Figure 5c. Permanent scatterer velocity map from ENVISAT data for the period 18 April 2003 to 27 May 2005 and water-level change for the period April 2003 to May 2005.

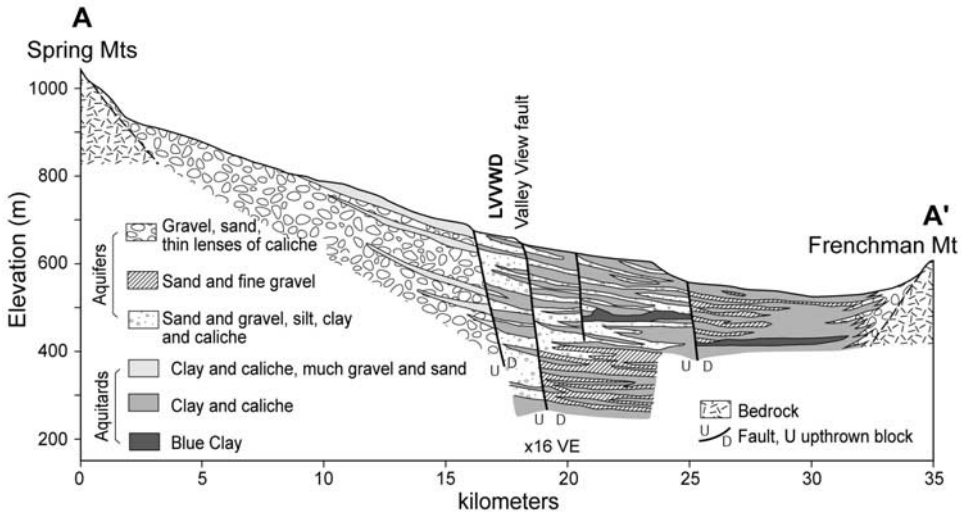

Figure 6. Diagrammatic hydrostratigraphic section through Las Vegas Valley (after *Maxey and Jameson* [1948]) showing abrupt change from western aquifers to eastern aquitards across the Valley View fault; see Figure 3 for location of section. LVVWD: Las Vegas Valley Water District main well field.

water levels have risen by more than 30 m (Figure 2b). These offsets are likely attributable to the differing thickness and hydraulic properties of the aquifers and aquitards underlying these areas, which change abruptly across the Valley View fault (Figure 6). Most of the pumping and artificial recharge occurs within gravelly, poorly compressible sediments of the principal aquifers lying to the west of the Valley View fault, and most of the aquifer-system compaction and recovery is occurring in the compressible aquitard section to the east of the Valley View fault. The aquitards are responding to fluid pressure changes within the adjacent pumped aquifers providing some insights into the bulk skeletal storage properties of the entire aquifer system (discussed further below).

[26] The linear zone of maximum uplift (5–10 mm/a) that extends from the Valley View fault north to the Eglington fault on the 2003–2005 data (Figure 5c) is unusual. Hydrogeologic characteristics of the aquifer system are relatively uniform through this part of the study area [*Morgan and Dettinger*, 1996], so the reason for this linear recovery pattern is not known. One possible explanation is that the feature is controlled by unrecognized structure, with an extension of the Valley View fault possibly influencing rising hydraulic heads.

[27] Although there is a general spatial association between rising water levels and uplift, we cannot completely preclude the possibility that the shortening of radar LOS distance that we are attributing to uplift may also reflect an undetected horizontal displacement component. Because the look angle of the ERS acquisitions is steep but not vertical ($\sim$23°), a small horizontal displacement may be present but go undetected without additional data analysis [*Hoffmann and Zebker*, 2003]. It is well known that horizontal hydraulic strains are generated by heavy pumping [*Helm*, 1994], and such strains are believed responsible for the formation of earth fissures near faults in Las Vegas Valley [*Burbey*, 2002]. The small area of uplift seen near the Eglington fault in the 1992–1996 time period is a well-known fissure zone [*dePolo and Bell*, 2002] indicating that horizontal strain has occurred at some time in this area. Horizontal deformation associated with heavy pumping has been observed with InSAR in other heavily pumped basins [*Gourmelen et al.*, 2007], and additional studies utilizing lower-look-angle acquisitions would be necessary here to differentiate a horizontal component.

6.3. Seasonal Aquifer-System Response

[28] Seasonal aquifer-system response measured by conventional InSAR has been previously reported in Las Vegas Valley [*Hoffmann et al.*, 2001] and in other groundwater basins of the western US [*Lanari et al.*, 2004; *Schmidt and Burgmann*, 2003]. In this study we utilized PSInSAR™ to analyze in greater detail the spatial and temporal patterns associated with seasonal response than allowed by conventional InSAR.

[29] Most PS targets exhibit a seasonal signal superimposed on a long-term trend, including the areas showing recovery and uplift (see Figure 7). In order to discern patterns of seasonal response, we segregated the seasonal signals by magnitude and time of year. To determine maximum seasonal amplitudes, we first subtracted the known, linear, long-term trend from each time series and then fit a sinusoidal model to each de-trended time series:

$$Y(t) = Y_0 + \mathrm{Amp} * \cos(2\pi(t - T)) \quad (1)$$

where Amp is the maximum seasonal amplitude (mm) for either subsidence or uplift oscillations, T is time of year of the maximum amplitude, and Y_0 accounts for a constant shift in the model due to interferometric noise and artifacts. The linear trend (Figure 9a) is removed from the time series and a sinusoidal model is fit to the residual for each time series (Figure 9b). For the seasonal analysis we assume a 1-year periodicity for the ground movement based on the annual cycles of pumping and recharge.

[30] The seasonal model was fit to each target in a 1995–1998 ERS data subset which contains the most robust seasonal data points. Each time series was first filtered by

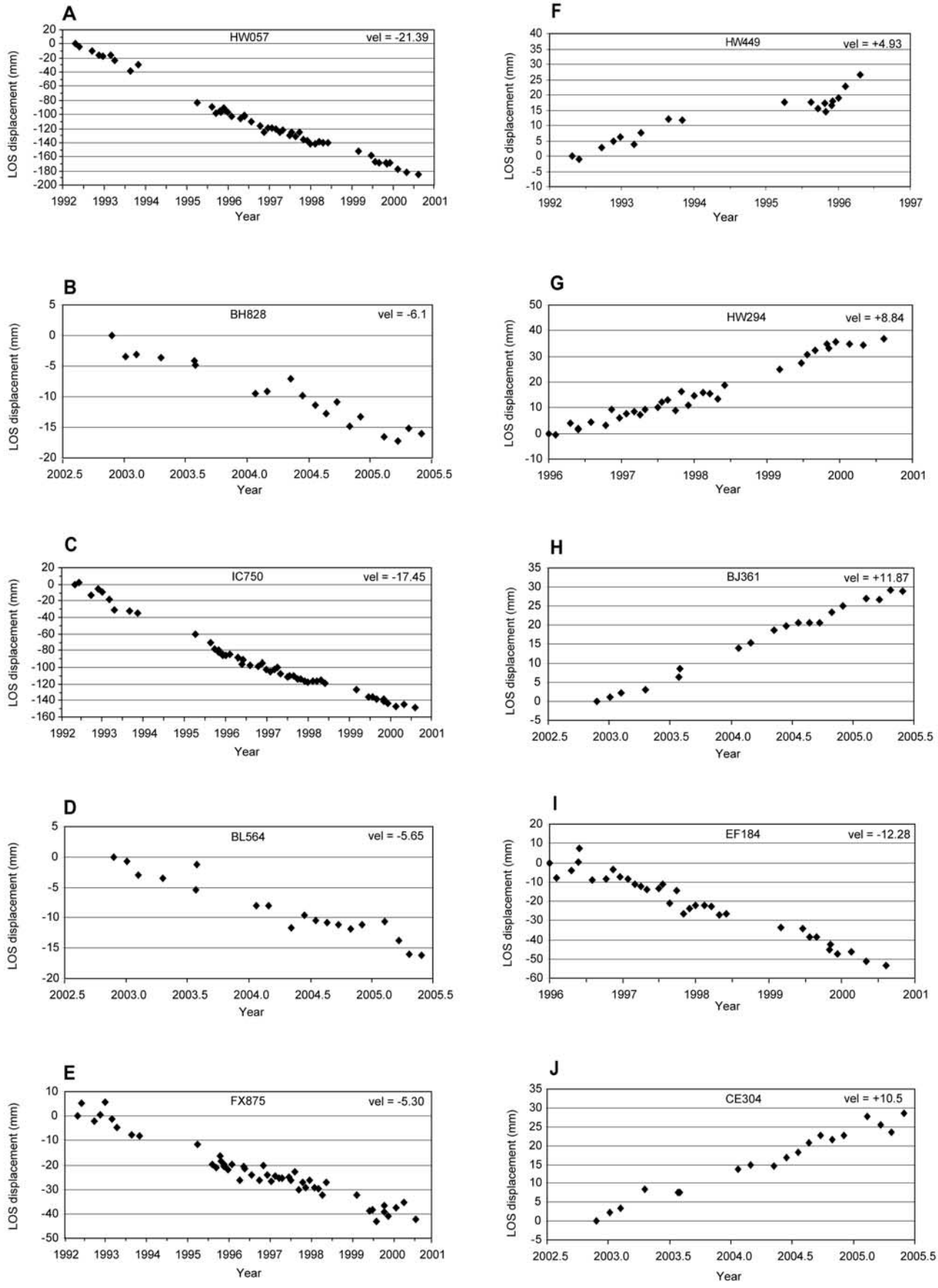
A
HW057
vel = -21.39
B
BH828
vel = -6.1
C
IC750
vel = -17.45
D
BL564
vel = -5.65
E
FX875
vel = -5.30
F
HW449
vel = +4.93
G
HW294
vel = +8.84
H
BJ361
vel = +11.87
I
EF184
vel = -12.28
J
CE304
vel = +10.5
LOS displacement (mm)
Year

Figure 7

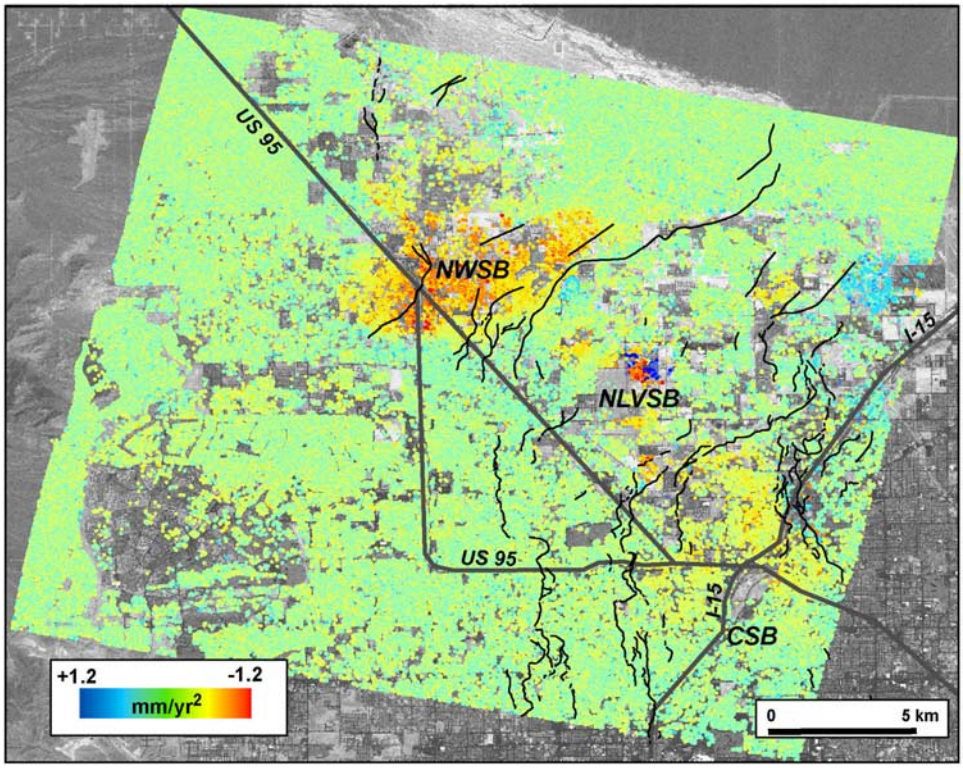

Figure 8. Acceleration/deceleration map derived from comparison of 1992–1996 and 1996–2000 PS time series data. The Northwest subsidence bowl (NWSB) exhibits residual subsidence that is decelerating at a rate of ~1 mm/a^2, while the North Las Vegas subsidence bowl (NLVSB) and the Central subsidence bowl (CSB) are nearly stable. Faults shown in black.

averaging all PS targets within a 500-m radius in order to reduce noise and to highlight areas of most active seasonal response. The model parameters were determined using a standard Least Mean Squares estimation, and the results were then sorted by maximum amplitude (either subsidence or uplift) and time of year to look for spatial and temporal patterns.

[31] The results show that the maximum seasonal response is clustered in four areas (Figure 10a). Area 1 is located at the northern margin of the Northwest subsidence bowl near a spring zone; area 2 is located immediately east of the Las Vegas Valley Water District main well field; area 3, which exhibits the largest seasonal amplitudes, is located in the Central subsidence bowl; and area 4 is located at the eastern margin of the North Las Vegas subsidence bowl adjacent to a new golf course. The reasons for the occurrence of these clusters and the spatial distribution are not entirely clear. On the basis of the location of the artificial recharge wells, only area 2 adjacent to the Las Vegas Valley Water District has a close spatial association with a recharge zone; the other clusters are 5–10 km from the nearest recharge well. However, area 4 is adjacent to new golf course wells that began pumping in 1997 (Bruce Wert, written commun., 2007), and it is the only area that exhibits an acceleration in the subsidence rate (Figure 8). Each of these maximum seasonal amplitude clusters occurs in an area underlain by thick sections of fine-grained deposits [*Plume*, 1984; *Morgan and Dettinger*, 1996]. Therefore we infer that the seasonal clusters are related to elastic response of sediments within the compressible aquitard sequence. This observation, however, appears to conflict with the general concept that fine-grained aquitards will be slow to respond to head changes (discussed further in section 6.4). The rapid seasonal response observed here therefore suggests that the aquitard section probably contains some beds of fine-grained aquifers, or more compressible aquifers, than generally believed which contribute to the rapid response.

[32] The results further show a temporal clustering of the maximum amplitudes in the Spring of each year for areas 1–3 (Figure 10b). Strong seasonal uplift components are found in the time series oscillations with a seasonal uplift response occurring in the Spring; a corresponding seasonal subsidence oscillation may occur six months later but it cannot be determined directly from the model. The uplift component is related to the effects of the annual artificial recharge, and the subsidence component would be related to the annual pumping. Because the sinusoidal model assumes

Figure 7. PS time series for selected subsiding and uplifting data points (PS target name on each chart), with calculated average, long-term point velocities (mm/a) determined by linear regression of the time series. See Figures 5a, 5b for location of PS data points identified by charts A-J.

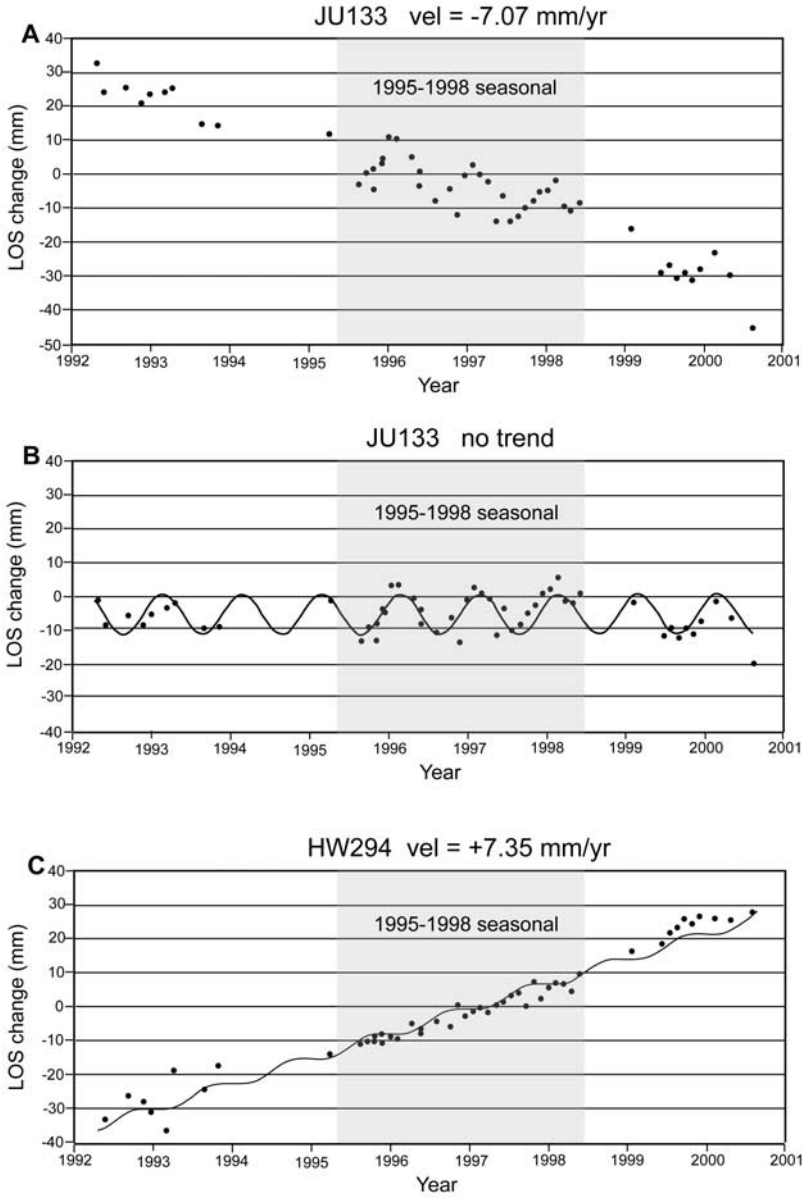

Figure 9. Illustrative example of seasonal model application incorporating maximum seasonal amplitude and time of year for each PS target. (a) PS target JU133 time series for 1992–2000 showing linear subsidence trend of −7.07 mm/a; point K located on Figure 5b. (b) Seasonal sinusoidal model fit to target K time series results after removal of long-term subsidence trend. (c) Seasonal model fit to uplifting target G (Figures 5b, 7) showing seasonal uplift signal superimposed on long-term linear uplift of +7.35 mm/a.

that maximum seasonal uplift and subsidence amplitudes are of equal magnitude, we thus cannot determine the dominant oscillation, if any.

[33] The maximum seasonal amplitude clusters in areas 1, 2, and 3 occur during the January through March period of each year, indicating that a maximum seasonal oscillation is associated with the final stages of artificial recharge, which typically begins in late October and ends in late March of each year. In area 2, a small cluster subset occurs in early April at the actual end of the recharge period. It is interesting to note that areas 1 and 3 are responding closely to seasonal recharge although spatially separated from the recharge wells, suggesting that elastic response to recharge is quite rapid throughout the aquifer system.

[34] Seasonal signals are also superimposed on the larger uplift trends for some data points in the aquitard sequence (Figure 9c), indicating that there are both short- and long-term components to the elastic response. As the aquitards are expanding elastically due to long-term water-level recovery, they are also responding seasonally to annual pumping and recharge. As noted above, we speculate that the rapid seasonal response within the aquitard sequence may be due to the presence of fine-grained beds that respond like elastic aquifers.

[35] The seasonal cluster adjacent to the Las Vegas Valley Water District (Figure 10a, area 2) is located on the east side of the Valley View fault, a structural discontinuity in the aquifer system underlying the well field and separating the highly transmissive pumped aquifers to the west from the compressible aquitards to the east (Figure 6). On the basis of Figure 10a, the east side of the fault (PS target JG901) exhibits an average 2–3 mm maximum seasonal amplitude superimposed on a long-term subsidence trend of ~4 mm/a (Figure 11a). The west side of the fault (PS target JG963) shows no significant long-term subsidence trend (Figure 11b), and a smaller (<2 mm), seasonal signal is present, further supporting the observation that the aquitards appear to be more responsive to both seasonal and long-term head changes. Comparing both seasonal uplift signals to the seasonal water-level fluctuations in the well field,

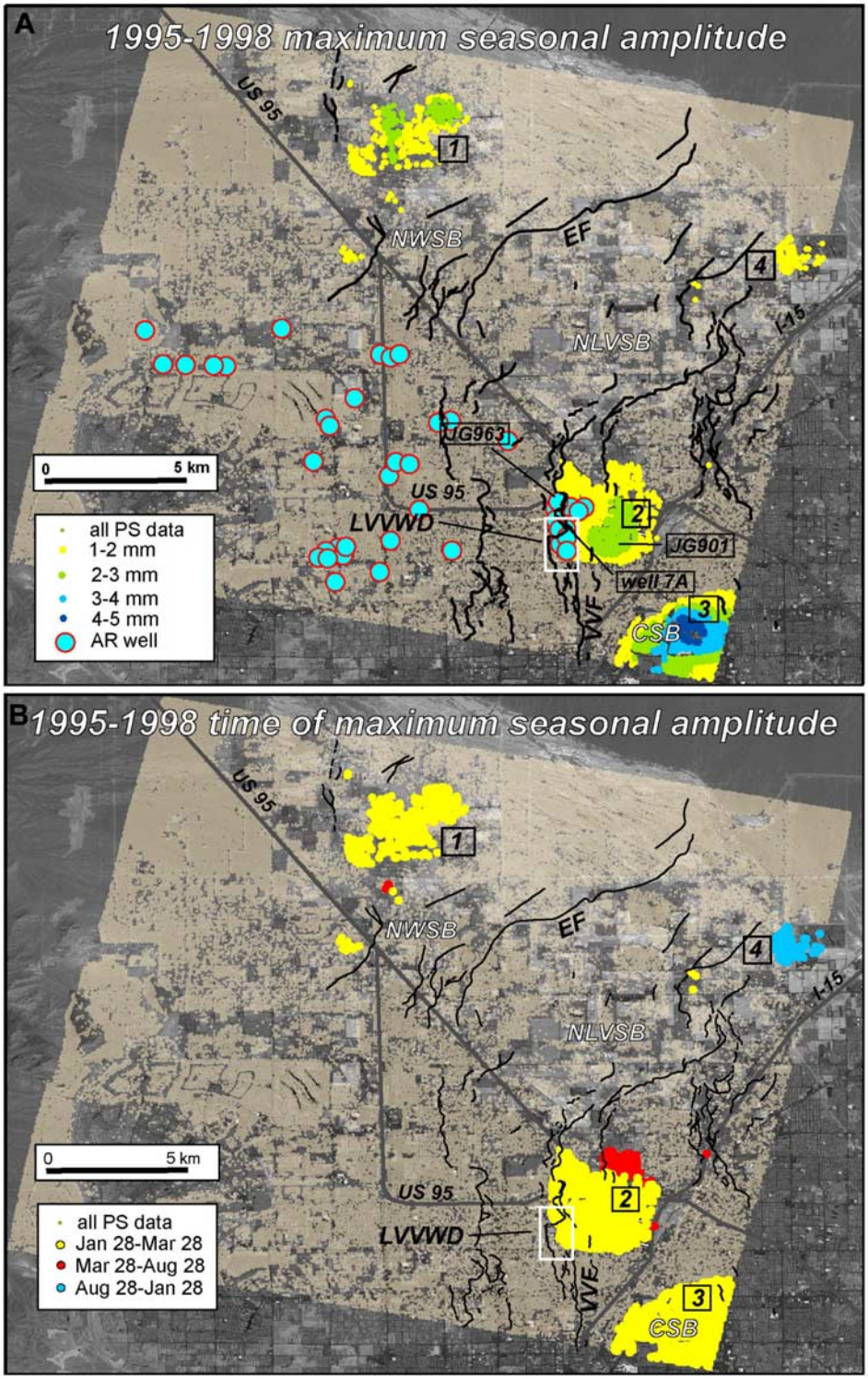

Figure 10

here using a representative water-level record from well 7A, the seasonal signals are coincident with rising and declining water levels. A time lag between water-level change and seasonal response, if any, is not evident. These results further support the conclusion that the seasonal (elastic) response of the aquifer system in general to water-level change is rapid.

6.4. Aquifer Storage Properties Derived From PSInSAR™

[36] Permanent subsidence in unconsolidated basin-fill aquifer systems such as Las Vegas Valley is caused not simply by declining artesian heads and compaction of coarse-grained aquifers, but primarily by nonrecoverable compaction of aquitards (low permeability, compressible fine-grained deposits) owing to head (groundwater level) declines in the adjacent aquifers [*Morgan and Dettinger*, 1996; *Galloway et al.*, 1998; *Hoffmann et al.*, 2001]. This process is generally referred to as the aquitard-drainage model [*Tolman and Poland*, 1940; *Helm*, 1984]. In this model, the aquifer system consists of aquitards interbedded with, or adjacent to, the aquifers, and as hydraulic heads are lowered in the aquifers, the effective stress in the aquitards increases and compaction occurs as they are drained. Groundwater flows from the aquitards as the hydraulic heads in the aquitards equilibrate with the head changes in the adjacent aquifers. The delayed drainage element of the aquitard-drainage model predicts that residual subsidence will account for part of the ultimate compaction of the system [*Helm*, 1984].

[37] Subsidence in the Las Vegas Valley aquifer system is best characterized by the aquitard-drainage model. The pumped aquifers are poorly compressible, and historically a significant component of the pumped groundwater in the basin comes from water released from storage during the compaction of the fine-grained aquitards [*Morgan and Dettinger*, 1996]. While the aquifers will respond elastically to head declines accompanying pumping, the aquitards will respond both elastically and inelastically depending upon whether the maximum preconsolidation stresses are exceeded as the head declines propagate into the aquitards; with long-term water-level decline and inelastic compaction, the aquitards will continue to exhibit delayed drainage and residual compaction even though heads in the adjacent aquifers may have recovered. Such delayed drainage is evident in the pattern of residual subsidence found in this study.

[38] Compaction of the aquitards is controlled by effective stress relations for poroelastic media [*Terzaghi*, 1925]. The total stress, σ_T, for any given layer in the aquifer system is equal to the sum of the effective stress, σ_e, and the pore pressure, μ_w:

$$\sigma_T = \sigma_e + \mu_w \tag{2}$$

If the total stress in the system remains constant, a change in pore pressure will result in an equal and opposite change in effective stress. Deformation of the aquifer system due to changes in effective stress, $\Delta\sigma_e$, is primarily related to the compressibility of the aquifer-system skeleton, described by the skeletal storage coefficient, S_k^*, a bulk value representing the combined skeletal response of both aquifers (S_k) and aquitards (S'_k) [*Hoffmann et al.*, 2001]:

$$S_k^* = S_k + S'_k \tag{3}$$

In Las Vegas Valley, inelastic storage coefficients may be up to 30 times larger than elastic storage coefficients [*Morgan and Dettinger*, 1996]. Because skeletal compaction of the aquifers is primarily elastic and recoverable, a principal benefit of determining S_k^* values lies in the ability to characterize the inelastic storage properties of the aquitards. Aquitards can deform both elastically and inelastically, and the aquitard skeletal storage is described by two components depending on whether the maximum preconsolidation stress ($\sigma_{e\ \max}$) is exceeded:

$$S'_{ke} = \alpha_{ke}\rho g \mathrm{b} \qquad \sigma_e \le \sigma_{e\ \max} \tag{4}$$

$$S'_{ki} = \alpha_{ki}\rho g \mathrm{b} \qquad \sigma_e > \sigma_{e\ \max} \tag{5}$$

where $\alpha_{ke\ \text{and}}\ \alpha_{ki}$ are the elastic and inelastic skeletal compressibilities, ρ is the density of water, g is gravitational acceleration, and b is aquifer-system thickness.

[39] If the effective stress changes ($\Delta\sigma_e$) are due only to pore pressure changes ($\Delta\mu_w$) with constant total stress, it can be shown that the bulk elastic and inelastic storage coefficients (S_{ke}^* and S_{ki}^*) can be estimated by relating the change in aquifer-system thickness or compaction (Δb) to the change in effective stress ($\Delta\sigma_e$), reflected by the change in hydraulic head (Δh) [*Hoffmann et al.*, 2001]:

$$S_{ke}^* = \Delta \mathrm{b}_e / \Delta\ \mathrm{h}_e \tag{6}$$

$$S_{ki}^* = \Delta \mathrm{b}_i / \Delta\ \mathrm{h}_i. \tag{7}$$

The bulk inelastic skeletal storage estimate (equation (7)) assumes that the measured compaction is the ultimate compaction for the measured head change, that is, the heads

Figure 10. Spatial and temporal clustering patterns of maximum seasonal amplitudes derived from application of seasonal sinusoidal model to all PS targets, after spatial filtering. (a) Maximum seasonal amplitudes color-coded by size (mm). Four clusters (1, 2, 3, and 4) are present with the largest amplitudes located in cluster 3 in the Central subsidence bowl. Location of artificial recharge (AR) wells shown by blue circles. PS targets JG963 and JG901 occur on the west and east sides, respectively, of the Valley View fault (VVF) and well 7A is located within the Las Vegas Valley Water District main well field (LVVWD). (b) Time of maximum seasonal amplitudes shown in A color-coded by time of year. Nearly all maximum amplitudes (clusters 1, 2, and 3) occur in late March during the late stages of artificial recharge, indicating that the maximum amplitudes are related to elastic aquifer-system recovery and uplift. Area 4 shows maximum seasonal amplitudes occurring in late summer, indicating that seasonal response in this area is related to pumping.

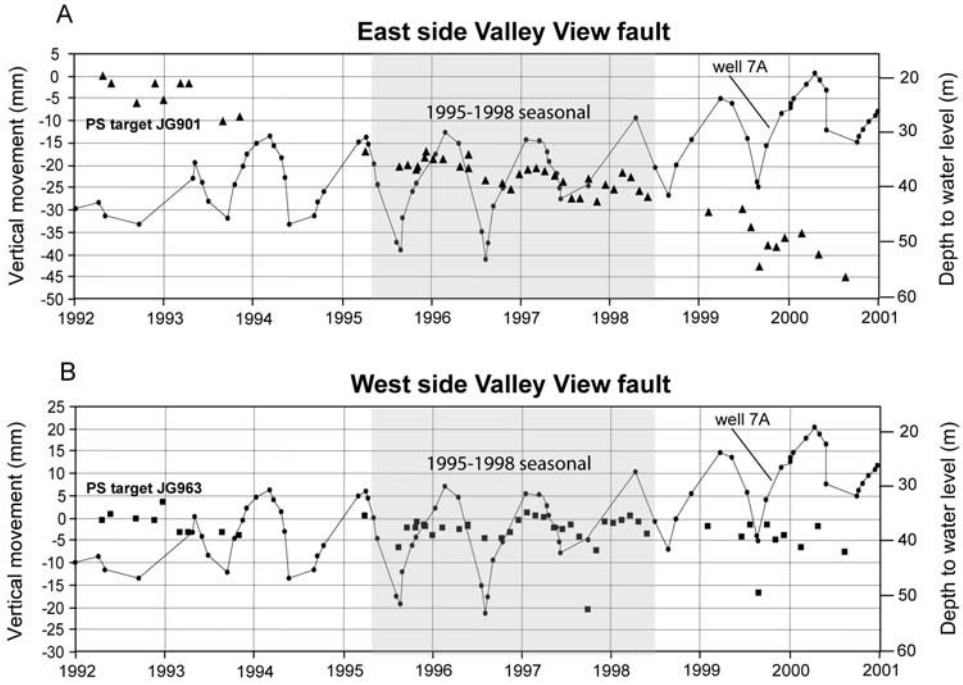

Figure 11. Comparison of seasonal and long-term trends for PS targets JG901 and JG963, which straddle the Valley View fault, with the water-level changes recorded in LVVWD well 7A; see Figure 10a for locations. The best comparisons are made for the 1995–1998 period which show a close correlation between seasonal water-level fluctuations and elastic response of both targets. (a) Time series for PS target JG 901 located in the aquitards on the east side of the Valley View fault; time series shows long-term subsidence rate of ~4 mm/a and 2–3 mm seasonal amplitudes. (b) Time series for PS target JG963 located in the aquifers on the west side of the Valley View fault; time series shows little long-term subsidence and 1–2 mm seasonal amplitudes.

governing compaction in the aquitards are fully equilibrated with the head changes measured in wells.

[40] Here we employ the approach of *Hoffmann et al.* [2001] and illustrate that by utilizing the PS time-displacement data set with corresponding water-level change data we can estimate the bulk elastic (S^*_{ke}) and inelastic (S^*_{ki}) skeletal storage coefficients with high spatial density and accuracy. The change in aquifer-system thickness or compaction (Δb) is the LOS displacement (assumed to be vertical) derived from InSAR results, and the change in effective stress ($\Delta\sigma_e$) is reflected by hydraulic head or water-level change (Δh). In contrast to earlier conventional InSAR-derived data sets, our PS time series allows recognition and differentiation of the seasonal and long-term deformation signals.

[41] Although the PS data set begins in 1992, it can be compared with earlier conventional geodetic data in order to estimate inelastic storage coefficients in the active Northwest subsidence bowl where water levels continued to decline during the study period. PS targets A and B on Figure 5a are located in the most active portions of the Northwest bowl, an area that had a maximum measured displacement of 150 cm between 1963–1990 [*Bell et al.*, 2002]. The PS results show that S^*_{ki} values for the aquitard section underlying the Northwest bowl are in the range of 9.0×10^{-3}–2.0×10^{-2} (Table 1), in good agreement with values derived from conventionally measured displacements and with model estimates for Las Vegas Valley [*Morgan and Dettinger*, 1996]. For example, vertical-control data from USGS benchmark R169 show that 130 cm of subsidence occurred between 1963–1990 as water levels declined by 75 m, yielding a long-term inelastic storage coefficient (S^*_{ki}) of 1.7×10^{-2}. The PS data for target C located at the R169 site show 9 cm of subsidence between 1992–1996 when water levels declined 5 m, yielding a similar S^*_{ki} value of 1.8×10^{-2}.

[42] Although other portions of the study area generally do not allow estimates of S^*_{ki} values to be made because of the rising water levels, several monitored well sites do provide estimates of S^*_{ke} values measured by PS displacements and rising water levels in the wells. As noted, the North Las Vegas bowl exhibits a reversal of aquifer-system compaction since 2003, and comparable uplift rates are present in the Eglington fault area beginning in the 1992–1996 period. The elastic S^*_{ke} values estimated from PS data for these areas are in the range 2.0–3.7×10^{-3}. These results are in agreement with those of *Hoffmann et al.* [2001] who used conventional InSAR to determine S^*_{ke} for six well sites where they found values ranging between 4.2×10^{-4} to 3.4×10^{-3}. The results also agree with *Morgan and Dettinger* [1996] whose model estimated elastic storage coefficients to be in the range of 1.0×10^{-3} to 3.0×10^{-3} for the aquifer system in general.

[43] The storage coefficient results for the Eglington fault uplift area, however, are anomalous based on the longer-term subsidence record. Historical benchmark data indicate that less than 30 cm of compaction has occurred in this area despite a 45 m decline in water levels, yielding an inelastic

Table 1. Ground Displacements Measured by Historical Data (H) and PS Targets (PS), With Water-Level Change, Used to Calculate Selected Inelastic (S^*_{ki}) and Elastic (S^*_{ke}) Storage Coefficients

Time Period	Subsidence/Uplift, cm	Velocity, cm/yr	Water-Level Change, m	S^*_{ki}; S^*_{ke}
		Northwest subsidence bowl		
		Zone of maximum subsidence; PS target HW 057		
1963–1990 (H)	−150	−5.5	−60–75	S^*_{ki} 2.0–2.5 × 10^{-2}
1992–1996 (PS)	−10	−2.7		−5 S^*_{ki} 2.0 × 10^{-2}
1996–2000 (PS)	−8	−1.8	+5	–
		Benchmark R169; PS target IC 750		
1963–1990 (H)	−130	−4.8	−75	S^*_{ki} 1.7 × 10^{-2}
1992–1996 (PS)	−9	−2.2	−5	S^*_{ki} 1.8 × 10^{-2}
		Painted D well; PS target IH280		
1963–1990 (H)	−150	−5.5	−60–75	S^*_{ki} 2.0–2.5 × 10^{-2}
1992–1996 (PS)	−5	−1.2	−5.3	S^*_{ki} 9 × 10^{-3}
		North Las Vegas subsidence bowl		
		Simmons well; PS targets IN 753, CE 304		
1963–1990 (H)	−60	−2.2	−45	S^*_{ki} 1.3 × 10^{-2}
1996–2000 (PS)	−2.5	−0.6	+12.6	–
2003–2005 (PS)	+2.0	+1.0	+5.3	S^*_{ke} 3.7 × 10^{-3}
		Eglington fault area		
		Willis/Silver Mesa wells; PS targets HS 449, BG378, HT525		
1963–1990 (H)	−15–30	−0.5–1.0	−45	S^*_{ki} 3.3–6.6 × 10^{-4}
1992–1996 (PS)	+2.5	+0.25	+1.5	S^*_{ke} 1.7 × 10^{-2}
1996–2000 (PS)	+2.0	+0.5	+9.4	S^*_{ke} 2.0 × 10^{-3}
2003–2005 (PS)	+1.0	+0.5	+4.9	S^*_{ke} 2.0 × 10^{-3}
		Central subsidence bowl		
		Dr. Park well; PS targets FX 875, FX 807, DI 931		
1963–1990 (H)	−60	−2.2	−30	S^*_{ki} 2.0 × 10^{-2}
1992–1996 (PS)	−3.0	−0.75	+1.4	–
1996–2000 (PS)	−1.5	−0.5	+3.4	–
2003–2005 (PS)	−0.8	−0.2	+1.4	–

S^*_{ki} value significantly less than the S^*_{ke} values derived from the PS data. This may be a further indication that the PS uplift signal is in part attributable to undetected horizontal motion.

7. Conclusions

[44] This study used the PSInSAR™ methodology together with detailed water-level change data for the first time to examine the temporal and spatial pattern of seasonal and long-term aquifer-system response to pumping and artificial recharge in Las Vegas Valley, providing insights into important aspects of the system response that can form the basis for similar studies in other heavily pumped groundwater basins.

[45] Temporal PS data sets reveal that long-term aquifer-system response has been strongly influenced by the continued rise of water levels resulting from the artificial recharge program initiated in the late 1980s. Time series velocities show that subsidence has been decreasing in rate since 1996, and that in some areas it has been completely arrested and locally reversed. Residual subsidence of as much as 5 mm/a, however, is continuing in the principal subsidence bowls even though water levels have risen more than 25 m during the same period. In the Northwest subsidence bowl, PS data show that velocities have been decelerating at a rate of about 1 mm/a^2, decreasing from more than 3 cm/a to less than 1 cm/a.

[46] A comparison of time series velocity data shows that although subsidence velocities have been decelerating, residual compaction is continuing in some areas despite more than 10 years of recovering water levels, providing some measure of the time delay in aquitard drainage. On the basis of results for 2003–2005, residual subsidence in the Northwest subsidence bowl will continue for at least 5–10 years at the present deceleration rate.

[47] The 2003–2005 PS results show that the long-term rise in water levels has resulted in extensive elastic aquifer-system recovery. A broad area of uplift exhibiting velocities of as much as +1 cm/a lies adjacent to the eastern margin of the principal artificial recharge zone, and subsidence has been reversed in portions of the North Las Vegas subsidence bowl. Although we cannot completely preclude the possibility that some of this apparent uplift signal is related to undetected horizontal aquifer displacement which would produce a similar radar LOS change, the temporal association of uplift with progressively rising water levels is supportive of an elastic recovery interpretation.

[48] The PS results illustrate that the aquifer-system response in Las Vegas Valley is complex. The principal areas of both seasonal and long-term aquifer system response are underlain primarily by thick sections of compressible aquitards; these areas are spatially offset from the principal areas of pumping and recharge that occur within the highly transmissive but poorly compressible aquifers. This relation suggests that aquifer-system response is largely driven by hydraulic pressure equilibrations in the aquitard section as pumping and recharge occurs in the adjacent aquifers.

[49] A sinusoidal model fit to each PS time series found that seasonal response is focused in four distinct clusters that show maximum uplift oscillations occurring primarily in the Spring of each year. The uplift oscillations coincide with the late stages of artificial recharge typically occurring in late March, indicating that seasonal uplift is a strong component of the annual seasonal oscillations. Because the model assumes that seasonal uplift and subsidence are of equal magnitude, we cannot determine if uplift is the dominant effect. The seasonal oscillations are superimposed on the longer-term subsidence patterns, as well as on the multiyear uplift trends, indicating that both short-term and long-term elastic recovery is occurring.

[50] Given the fact that there may be simultaneous compaction and expansion occurring as water levels recover in previously subsiding areas and seasonal response is superimposed on residual subsidence, exact estimates of storage coefficients are limited by the relative contributions of each response. For example, we calculated inelastic storage coefficients only at sites exhibiting water-level declines, and we assumed no residual compaction was occurring. In actuality, the magnitude of residual subsidence is not fully known, and we cannot preclude the possibility that we are overestimating the inelastic storage coefficients. Similarly, elastic storage coefficient estimates in those areas which had been subsiding and which now exhibit water-level rise and uplift may be underestimated if residual compaction is occurring simultaneously.

[51] Within the limitations of the uncertainties derived from the relative contributions of the seasonal and long-term, residual aquifer-system response, PS analysis provides the capability of differentiating an elastic seasonal response from the long-term inelastic response in order to estimate hydraulic properties of the system, namely the bulk skeletal storage coefficients. Here we used PS data to refine estimates of the seasonal elastic storage coefficients as well as to add new estimates of the long-term inelastic storage coefficients. We found that in order to accurately estimate the elastic storage coefficients, it was necessary to use multiyear trends, particularly in those areas where the seasonal uplift signal is superimposed on a longer-term uplift signal. Such analyses provide the basis for additional work that could characterize the storage properties of the entire aquifer system at a high degree of spatial resolution, and when combined with water-level and hydrostratigraphic data could produce a detailed analysis of storage coefficient variability, a study which is beyond the scope of the current study.

[52] This prototype study demonstrates that PSInSAR™ is a robust, high-resolution, widely applicable methodology that improves upon conventional InSAR methodologies by providing the capability to more fully characterize temporal and spatial patterns of aquifer-system response. It could be further improved by increasing the sampling frequency and by combining data from different SAR viewing geometries and multiple satellites, thereby allowing greater resolution of annual fluctuations of the seasonal signals and detection of horizontal aquifer displacements. We believe that this evolving methodology will provide an important new tool in future groundwater research and management that can be utilized in other heavily pumped groundwater basins throughout the western US and elsewhere. In addition, the permanent scatterer methodology may have broader applications to hydrologic research beyond groundwater resources, such as in the natural recharge in urban areas and in the system analyses of other ground fluid reservoirs, such as oil and gas.

[53] **Acknowledgments.** This study was supported by NASA Research Grant 13-02017 and European Space Agency Category-1 Research Grant C1P2636. The authors especially appreciate the assistance of Bruce Wert at the Las Vegas Valley Water District/Southern Nevada Water Authority who provided the water-level data. Borehole extensometer data through 2005 were provided by Mike Pavelko at the US Geological Survey, Las Vegas Field Office. Draft versions of the manuscript were reviewed by Scott Tyler, Joe Liesing, Bruce Wert, and David Donovan. The authors greatly appreciate the helpful manuscript reviews by Devin Galloway, Tom Burbey, and Chris Browitt.

References

Amelung, F., D. L. Galloway, J. W. Bell, H. A. Zebker, and R. J. Laczniak (1999), Sensing the ups and downs of Las Vegas: InSAR reveals structural control of land subsidence and aquifer-system deformation, *Geology*, *27*(6), 483–486.

Bell, J. W., F. Amelung, A. Ramelli, and G. Blewitt (2002), Land subsidence in Las Vegas, Nevada, 1935-2000: New geodetic data show evolution, revised spatial patterns, and reduced rates, *Env. Eng. Geosci.*, *VIII*(3), 155–174.

Burbey, T. J. (1995), Pumpage and water-level change in the principal aquifer of Las Vegas Valley, 1980-1990, *Nev. Dept. Conserv. Natural Resour.*, *Water Resour. Inf. Rep., 34*, 224 pp.

Burbey, T. J. (2002), The influence of faults in basin-fill deposits on land subsidence, Las Vegas, Nevada, USA, *Hydrogeol. J.*, *10*, 525–538.

dePolo, C. M., and J. W. Bell (2002), Map of faults and earth fissures in the Las Vegas area, *Nev. Bur. Mines Geol. Open-file, 01-4*.

Donovan, D. J., and T. Katzer (2000), Hydrologic implications of greater groundwater recharge to Las Vegas Valley, *J. Am. Water Resour. Assoc.*, *36*(5), 1133–1148.

Ferretti, A., C. Prati, and C. Rocca (2001), Permanent scatterers in SAR interferometry, *IEEE Trans. Geosci. Remote Sens.*, *39*(1), 8–20.

Ferretti, A., G. Savio, R. Barzaghi, A. Borghi, S. Musazzi, F. Novali, C. Prati, and F. Rocca (2007), Sub-millimeter accuracy of InSAR time series: Experimental validation, *IEEE Trans. Geosci. Remote Sens.*, *45*(5), 1142–1153.

Galloway, D. L., and J. Hoffmann (2006), The application of satellite differential SAR interferometry-derived ground displacements in hydrogeology, *Hydrogeol. J.*, doi:10.1007/s10040-006-0121-5.

Galloway, D. L., K. W. Hudnut, S. E. Ingebritsen, S. P. Philips, G. Peltzer, F. Rogez, and P. A. Rosen (1998), Detection of aquifer system compaction and land subsidence using interferometric synthetic aperture radar, Antelope Valley, Mojave Desert, California, *Water Resour. Res.*, *34*, 2573–2585.

Galloway, D., D. R. Jones, and S. E. Ingebritsen (Eds.) (1999), Land subsidence in the United States, *U.S. Geol. Surv. Circ., 1182*, 175 pp.

Gourmelen, N., F. Amelung, F. Casu, M. R. Manzo, and R. Lanari (2007), Mining-related ground deformation in Crescent Valley, Nevada, *Geophys. Res. Lett.*, *31*, L09309, doi:10.1029/2007GL029427.

Hanssen, R. (2001), *Radar interferometry, volume 2: Remote sensing and digital image processing*, 308 pp., Kluwer Academic Publishers, Dordrecht, Boston, London.

Helm, D. C. (1984), Field-based computational techniques for predicting subsidence due to fluid withdrawal, in *Man-induced land subsidence*, edited by T. L. Holzer, *Rev. Eng Geol.*, *VI*, The Geological Soc. of America, Boulder, 1–22.

Helm, D. C. (1994), Hydraulic forces that play a role in generating fissures at depth, *Bull. Assoc. Eng. Geol.*, *XXXI*(3), 292–304.

Hoffmann, J., and H. A. Zebker (2003), Prospecting for horizontal surface displacements in Antelope Valley, California, using satellite radar interferometry, *J. Geophys. Res.*, *108*(F1), 6011, doi:10.1029/2003JF000055.

Hoffmann, J., H. A. Zebker, D. L. Galloway, and F. Amelung (2001), Seasonal subsidence and rebound in Las Vegas Valley, Nevada, observed by synthetic aperture radar interferometry, *Water Resour. Res.*, *37*(6), 1551–1566.

Lanari, R., M. Lundgren, M. Manzo, and F. Casu (2004), Satellite radar interferometry time series analysis of surface deformation for Los Angeles, California, *Geophys. Res. Lett.*, *31*, L23613, doi:10.1029/2004GL021294.

Las Vegas Valley Water District (2005), 2005 Artificial recharge annual report, *Las Vegas Valley Water Dist. Unpub. Rpt*, 150 pp.

Maxey, G. B., and C. H. Jameson (1948), Geology and water resources of the Las Vegas, Pahrump, and Indian Springs Valleys, Clark and Nye Counties, Nevada, Nev. Dept. Conserv. Natural Resour., *Water Resour. Bull.*, *5*, 128 pp.

Morgan, D. S., and M. D. Dettinger (1996), Groundwater conditions in Las Vegas Valley, Clark County, Nevada, Part 2, Hydrogeology and simulation of groundwater flow, *U.S. Geol. Surv. Water Supply Pap. 2320-B*, 124 pp.

Pavelko, M. T. (2000), Ground water and aquifer-system compaction data from the Lorenzi Site, Las Vegas, Nevada, 1994-1999, *U.S. Geol. Surv. Open-file Rep. 00-362*, 26 pp.

Plume, R. W. (1984), Ground-water conditions in Las Vegas Valley, Clark County, Nevada, *U.S. Geol. Surv. Open-file Rep. 84-130*, 25 pp.

Schmidt, D. A., and R. Burgmann (2003), Time dependent land uplift and subsidence in the Santa Clara Valley, California, from a large InSAR data set, *J. Geophys. Res.*, *108*(B9), 2416, doi:10.1029/2002JB002267.

Terzaghi, K. (1925), *Principles of soil mechanics: IV, Settlement and consolidation of clay*, McGraw-Hill, New York, v. 95.

Tolman, C. F., and J. F. Poland (1940), Groundwater, salt water, infiltration, and ground surface recession in Santa Clara Valley, Santa Clara County, California, *Am. Geophys. Un.*, 23–34.

F. Amelung, Rosenstiel School of Marine and Atmospheric Science, University of Miami, Miami, FL, USA.

J. W. Bell, Nevada Bureau of Mines and Geology, University of Nevada, Reno, NV, USA. (jbell@unr.edu)

M. Bianchi, A. Ferretti, and F. Novali, Tele-Rilevamento Europa, Via Vittoria Colonna, 7, Milan, Italy.